ELSEVIER

International Journal of Mass Spectrometry 193 (1999) 161–179

International Journal of Mass Spectrometry

Stereochemical effects enhanced by using selective "self-ionization" under electron ionization conditions in a quadrupole ion trap mass spectrometer

E. Rathahao, M.C. Perlat, F. Fournier, J.C. Tabet*

Laboratoire de Chimie Structurale Organique et Biologique, UMR 7613 CNRS, Université Pierre et Marie Curie, 4 place Jussieu, 75252 Paris, Cedex 05, France

Received 12 February 1998; accepted 22 February 1999

Abstract

From a previous study on the reactivity of the *cis* and *trans* (4-hydroxy-4-methyl-cyclohexyl)-benzoates (Mw = 234) under ammonia chemical ionization conditions in high pressure source, it was demonstrated that competitive decompositions, have specific orientations. In particular, highly stereospecific benzoic acid loss from the *trans* isomer takes place, suggesting that protonation by NH_4^+ regioselectively occurred at the benzoate site rather than at the hydroxyl group. From the *cis* epimer elimination of water was only observed. This behavior could be explained by (1) possible proton transfer to both the functional groups and (2) decomposition occurring *via* water loss due to a higher rate constant compared with that of the benzoic acid loss ($PA_{C_6H_5COOH} > PA_{H_2O}$), which is not observed. These epimers are now studied under low pressure chemical ionization (CI) and electron impact (EI) conditions by using an ion trap mass spectrometer. Epimer differentiation from the stereospecific benzoic acid loss can be achieved independently of the gas-phase reagent used for chemical ionization, even if quasimolecular ions are entirely decomposed (i.e. in low pressure isobutane CI and methane CI). More spectacular differentiation is displayed in the ammonia CI mass spectra of epimers. Among the various quasimolecular species, the product $[MNH_4–H_2O]^+$ ions, termed substituted ions, usually containing a covalent $C–NH_3^+$ bond are herein in fact a noncovalent form similar to the ammonia solvating protonated(4-hydroxy-4-methyl-cyclohexyl)-benzoate structure, as shown by deuterium labeling. Other product ions such as $C_7H_{11}NH_3^+$ and $\{NH_3, C_6H_5COOH_2^+\}$ are detected in contrast to those observed under high pressure source conditions. Collision induced dissociation spectra of the adduct MNH_4^+ ions in addition to those of protonated molecules are investigated to obtain information about the location of ammonium (or proton) attachment. It appears for the *trans* isomer, a regioselective approach to the benzoate group, yielding $[MH–C_6H_5COOH]^+$, takes place rather than attack at the OH site resulting into $[MH–H_2O]^+$. This difference is at the origin of the observed stereospecific decomposition, which occurs *via* anchimeric assistance. Alternatively, these epimers give similar EI mass spectra, masking all the stereochemical effects, which reappear when using a residence time of 80 ms prior to apply the analytical scan. Under such conditions, ion–molecule reactions are enhanced, yielding formation of the epimeric MH^+ ions. These "*self-ionization*" processes are induced through exothermical proton transfers from many EI fragment ions. Competitive decompositions of the product even-electron MH^+ species provide a direct *cis*/*trans* differentiation. The diagnostic cleavages involved are comparable to those observed under low pressure CI conditions except that the loss of water occurs from both the precursors. The latter loss indicates that protonation is in competition and takes place at either of the basic sites, in contrast with that observed in chemical ionization. Furthermore, the exothermicity of proton transfer is preserved as internal energy of MH^+ which allows consecutive decompositions. At higher *m/z* ratio ranges, several adduct species are stereoselectively observed in the self-ionization mass spectrum of the *trans* epimer. These specific processes provide enhancement of the stereochemical *cis*/*trans* differentiation. (Int J Mass Spectrom 193 (1999) 161–179) © 1999 Elsevier Science B.V.

PII S1387-3806(99)00109-8

Keywords: Chemical ionization; Electron impact; Quadrupole ion trap; Stereochemistry

1. Introduction

Numerous investigations concerning stereochemical effects displayed on mass spectra have been reported [1,2]. In particular, positive ion chemical ionization (PICI) has been shown to be an efficient method for distinguishing diastereoisomers. This can be achieved by using a gas phase reagent [3–5] such as ammonia, methane, isobutane, and also more recently, dimethyl ether [6], borate [7], and phosphate [8]. Epimeric differentiation is noted from the change of the relative abundances of the quasimolecular ions as well as from the eventual fragment ions. Generally from monofunctional compounds, fragmentations of protonated MH^+ molecules are promoted by the charged group (e.g. as a nucleophilic site) [9], which is eliminated as a neutral during the dissociation processes.

Concerning fragmentation mechanisms of bifunctional protonated MH^+ molecules, they are more complicated since the eliminated group is not necessarily the one that is initially protonated as evidenced from several studies [10]. Indeed, if the functional groups are sterically blocked, strong interactions through hydrogen bonding may appear, leading to significant differences in diagnostic ion abundances displayed in PICI mass spectra of diastereoisomers. Then, the lost group may differ from the protonated one, which depends upon the proton affinity of the reagent gas [11] used. For instance, this behavior toward the NH_3/NH_4^+ system characterizes the reactivity of the *cis* 1c and *trans* 1t (4-hydroxy-4-methyl-cyclohexyl)-benzoate (Mw = 234 u) (Scheme 1) which displays stereospecific gas phase decompositions, i.e. losses of water and benzoic acid from 1c and 1t, respectively. This has been shown some years ago by using a reversed sector geometry mass spectrometer [12].

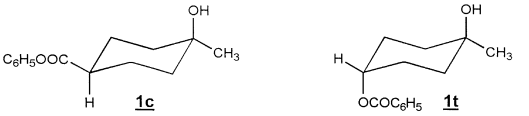

1c **1t**

Scheme 1. Structures of the *cis* 1c and *trans* 1t isomers of the (4-hydroxy-4-methyl-cyclohexyl)-benzoate.

It is expected that orientation of these dissociative pathways depends upon the respective proton affinity of the CI reagent used relative to that of the implied reactive site. Furthermore, the internal energy of the MH^+ ions is related to the proton transfer exothermicity and is influenced by the PA difference between those of the substrate and reagent. This internal energy modifies the unimolecular rate constants of the competitive decompositions, yielding particular orientations as well as the disappearance of the unstable MH^+ ions, which may be weakly observed in the chemical ionization (CI) mass spectrum.

In order to investigate the decomposition orientation of the protonated molecules toward the internal energy and protonated site, MH^+ ions have been prepared via "*self-ionization*" under electron impact (EI) conditions [13], providing competitive protonations at the benzoate and hydroxyl sites. These reactions have been performed by using a temporal mass spectrometer (e.g. ion trap mass spectrometer) [14]. This analytical technique is particularly effective because the reagent ions can be selectively stored according to a relatively large residence time. Modification of the reaction time to the optimized ion–molecule reaction responsible for MH^+ formation can be considered as an advantage of an ion trap mass spectrometer. The aim of the present study is the application of the self-ionization method for enhancing the 1c and 1t diastereoisomeric distinction compared to that provided from chemical ionization. In addition, stereospecific ion–molecule reactions will be investigated.

* Corresponding author.

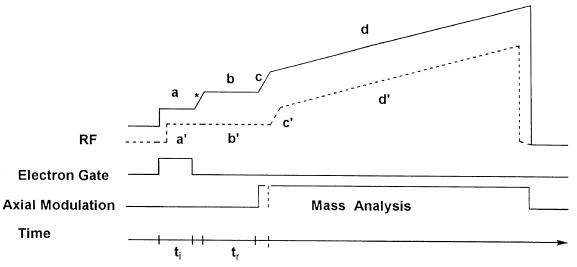

Fig. 1. Scan functions used for recording (a) CI ammonia mass spectra [a: reagent gas ionization followed by a waveform ejection of unwanted ions (asterisk); b: reaction of reagent ions with sample; c: ejection of ions with *m/z* ratio lower than that of the background *m/z* value; d: analytical scan, and (b) self-ionization mass spectra (a′: EI ionization; b′: delay time for enhancing ion–molecule reactions between EI fragment ions and sample neutrals; d′: analytical scan).

2. Experimental

2.1. Mass spectrometry

Experiments were performed on an ion trap mass spectrometer (Varian Saturn™ III, Walnut Creek, CA, USA) which operated with He buffer gas at $\sim 13.33 \times 10^{-2}$ Pa (i.e. 10^{-3} Torr). Revision C Software was used for data acquisitions in the full EI mass spectra, whereas a package software QISMS™, version 1.0 was employed for the construction of custom scan functions necessary to obtain particular training sequences for providing the self ionization and resonance absorption curves. EI mass spectra were obtained from injection of 1 μL of sample solution. The electron multiplier was biased at a voltage of 1800 V to reach a gain of 10^5 and the tunable target ion current for applying the automated gain control (AGC) algorithm was as 10 000 under self-ionization and ammonia CI conditions and chosen as 5000 under isobutane and methane CI conditions. Mass spectrum acquisition rate was 10 full scan, i.e. 50 microscans per mass spectrum. During the analytical scan step, 2 V_{o-p} amplitude of axial modulation (ω_z = 485 KHz); the analytical *m/z* ratio range was chosen as 30–500th (Fig. 1).

Fig. 1 displays the scan function used for recording *self-ionization* mass spectra, which has been applied to select reagent ions for introducing variable reaction times (t_r) and for optimizing variable amplitude excitation. The full *m/z* range was scanned without application of segmentation [15]. The low *m/z* ratio cutoff as 30th was chosen and corresponded to V_{o-p} = 307 V of the drive rf potential allowing ejection of ions provided from ionization of water and nitrogen present in the ion trap. Standard set conditions for recording mass spectra were: ionization duration and filament emission current respectively, 100 μs and 15 μA; ion trap temperature, 100 °C; reaction period, 65 ms for the chemical ionization ammonia (i.e. b step, Fig. 1) and 80 ms for self-ionization (i.e. c step, Fig. 1).

For selective ion excitation during sequential MS experiments, both the resonant and nonresonant excitation processes have been used for inducing the particular MH^+ dissociation. However, the consecutive decompositions (e.g. the *m/z* 217 → *m/z* 95 and *m/z* 113 → *m/z* 95 sequence occurring stereospecifically from the $\underline{1c}H^+$ and $\underline{1t}H^+$ epimeric ions, respectively) somewhat hindered observation of the stereospecific pathways. This factor prompted us to choose the resonant excitation mode relative to the second one. Indeed, under such conditions, dissociations related to weaker activation energy processes enhanced the stereochemical effects. The helium buffer gas ($\cong 13.33 \times 10^{-2}$ Pa) also served as the collision-induced dissociation (CID) target.

The scan function used by Saturn™ III under CID conditions is reported in Fig. 2 and represents temporal variation of various potentials applied to the different electrodes. During the ionization period A, the emission current was set at 15 μA and a preisolation multifrequency waveform having a frequency notch related to the secular frequency of the isolated ion was applied between the endcap electrodes in order to eject all undesirable ions. Period B corresponds, for each condition, to a variable reaction t_r time to produce ion–molecule reactions under *self-ionization* conditions between analytes and reactive fragment ions. In CI conditions, similar reaction times were used.

A finely tuned isolation was achieved by raising the rf amplitude in order to eject the remaining ions at *m/z* values lower than that of the isolated ion, and

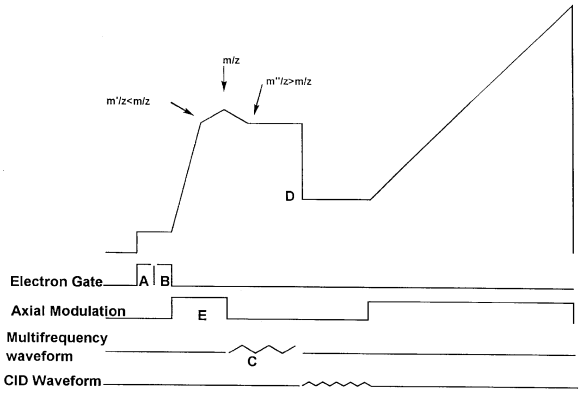

Fig. 2. Scan function used for recording CID mass spectra of selected precursor ions [a: ionization within t_i as time duration; b: variable reaction; t_r: delay time for producing ion–molecule reactions between analyte molecules and reactive IE fragment ions under self-ionization conditions; e: ejection of ions of lower *m/z* ratio than that of the isolated ion; c: broadband isolation step for ejection of ions with higher *m/z* ratios than that of the selected ion; d: location of the isolated ions in the stability diagram ($a_z = 0$; $q_z = 0.4$ as working points)].

during period C, by applying a multifrequency waveform (broadband isolation step) to eject ions having *m/z* values higher than that of an isolated ion *m/z*. In period D, lasting 5 ms, the rf amplitude was set in order to have a low *m/z* cutoff which located the isolated ion at the $a_z = 0$ and $q_z = 0.4$ working points. During this period, isolated ions were collisionally focused to the ion trap center through collisions with the buffer gas. The CID period was carried out by using a supplementary ac voltage (rf amplitude varied from 0.1 V_{o-p} to 1 V_{o-p}). The frequency $\omega_0 = 153.6$ kHz excitation related to the secular ion frequency found for $q_z = 0.4$ ($\beta_z = 0.2926$) was applied during 1.5 ms from which a maximum dissociation yield was reached.

A Varian star™ 3400 CX gas chromatography was used to introduce the sample solution in gas phase. The analytical GC column was a 30 m × 0.25 mm i.d. DB-5 fused silica capillary column. All samples were diluted with ethyl acetate (i.e. $c = 25 \times 10^{-6}$ to 0.3×10^{-3} g/mL) and 1 μL was injected in the splitless device (100 mL/mn). The transfer line was maintained at 230 °C, injector at 220 °C, and column temperature was maintained at 60 °C for 1 min; the

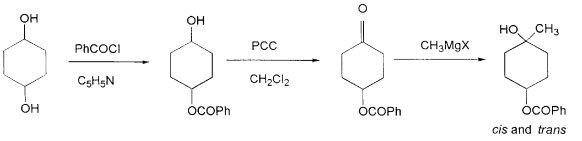

Scheme 2. Synthetic procedure of preparation of the 1c and 1t stereoisomers.

temperature was ramped at 30 °C/min to 150 °C; maintained at 150 °C for 1 min; ramped at 30 °C/min to 250 °C, which was stopped for 5 min at 250 °C. Under these experimental conditions, the (Z) and (E)(4-hydroxy-4-methyl-cyclohexyl)-benzoates eluated in 10.58 and 11.10 min, respectively. Helium pressure at the column head, as carrier gas, was 10 psi and was introduced as a cooling gas and also for providing CID processes.

2.2. Materials

The synthetic procedures used for the preparation of the studied diastereoisomers are outlined in Scheme 2. The Z and E-1,4-cyclohexanediol from Aldrich (10^{-3} mol) was converted into the monobenzoates by addition of benzoyl chloride (8.7×10^{-3} mol) in chloroform (10 mL), to a solution of the diol (8.6×10^{-3} mol) at 0 °C in pyridine (8 mL). The monobenzoates (6.76×10^{-3} mol) were then oxidized by the pyridinium chlorochromate (PCC) [9.96×10^{-3} mol in CH_2Cl_2 (10 mL)] to 4-benzoyloxycyclohexanone (yield: 85%) according to Corey method [16]. The produced ketone (2×10^{-3} mol) in anhydrous tetrahydrofurane (THF) (7 mL) was condensed with (2.8×10^{-3} mol) methylmagnesium iodid diluated in ether (3 *M*), and the *cis*/*trans* mixture of (4-hydroxy-4-methyl-cyclohexyl)-benzoate was obtained (yield: 21%) and purified by thin liquid chromatography (TLC) (eluant v:v ether/petrol ether 3:1; $Rf_{cis} = 0.57$; $Rf_{trans} = 0.39$).

3. Results

The epimeric (4-hydroxy-4-methyl-cyclohexyl)-benzoates are characterized by identical EI mass spectra displaying intense fragment ions without the

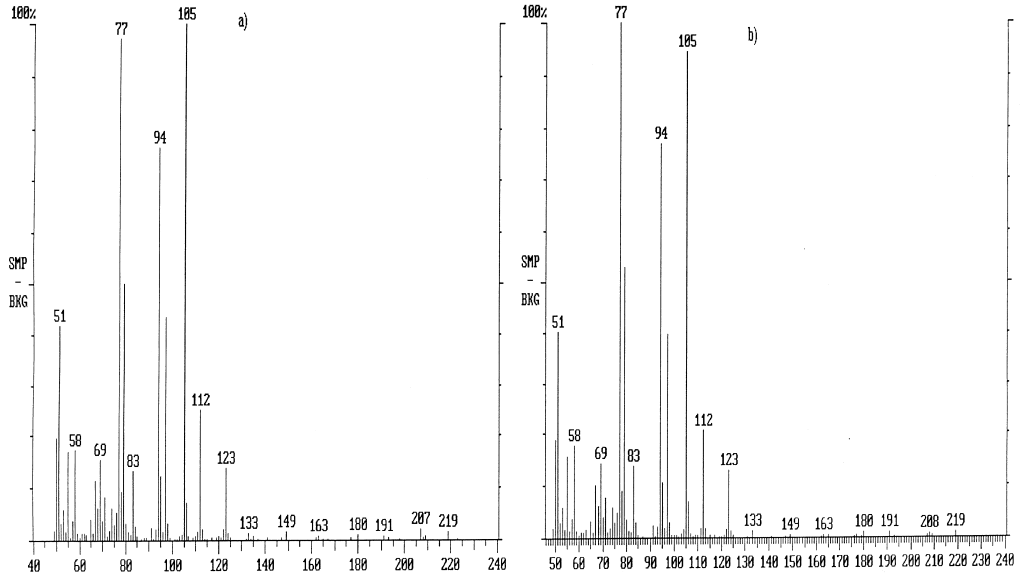

Fig. 3. EI mass spectra (without delay time prior to ion ejection) of the isomeric (a) *cis* and (b) *trans* of the (4-hydroxy-4-methyl-cyclohexyl)-benzoate (Mw = 234).

presence of molecular $M^{+\cdot}$ ions (Fig. 3). The numerous competitive and/or consecutive fragmentations hide the stereospecific decompositions. On the other hand, chemical ionization using methane and isobutane as gas phase reagents gives rise to formation of less numerous fragment ions as shown in Table 1. Stereospecific ions are observed at *m/z* 113, $[MH–C_6H_5COOH]^+$, and *m/z* 217, $[MH–H_2O]^+$, for 1t and 1c, respectively. Unfortunately, their relative abundances are less than 10% of the base peak in CI–CH_4.

Mainly, these ions dissociate by loss of water from *m/z* 113 and loss of benzoic acid from *m/z* 217 into the fragment *m/z* 95 ions, $[C_7H_{11}]^+$ (as the base peak). These consecutive decompositions are less extensive under isobutane CI conditions. From both the CI conditions, isomers lead to neither protonated molecules nor adduct ions. However, the *cis*/*trans* differentiation can be achieved based on the presence of the diagnostic peak at *m/z* 113 in spite of the absence of quasimolecular ions. Absence of the latter species reflects the particularly high internal energy of the MH^+ ions (*m/z* 235), which is due to the exothermicity of the protonation reaction.

A reverse trend characterizes the CI ammonia mass spectra of these epimers since the adduct ions and the protonated molecules are observed. They contain lower excitation energy because of a less exothermic proton transfer reaction. Under the latter conditions,

Table 1
Main ions displayed in the CH_4–CI and iC_4H_{10}–CI mass spectra of the isomeric *cis* and *trans* of the (4-hydroxyl-4-methyl-cyclohexyl) benzoate (Mw = 234) (ion abundances relative to the base peak).

		m/z 95	*m/z* 105	*m/z* 113	*m/z* 123	*m/z* 217
CI–CH_4	1c	100	6	. . .	5	4
	1t	100	5	8.8	9.5	. . .
CI–C_4H_{10}	1c	100	8.8	. . .	11	42.5
	1t	100	12.5	42.5	19.8	13.2

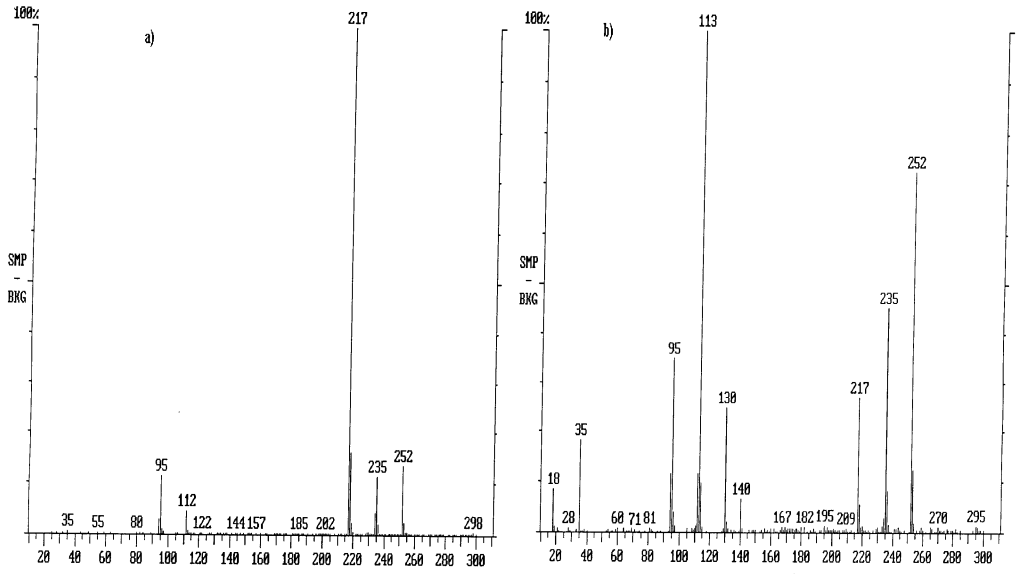

Fig. 4. CI ammonia mass spectra (without delay time prior to ion ejection) of the isomeric (a) *cis* and (b) *trans* of the (4-hydroxy-4-methyl-cyclohexyl)-benzoate recorded according to the procedure described in Fig. 1(a).

the stereochemical effects are enhanced as a showing of significant differences in abundances observed for the MNH_4^+ ions (*m/z* 252) as well as for the fragment *m/z* 113 ion, which appears as the diagnostic signal of the *trans* geometry (Fig. 4).

Finally, stereochemical effects have been also investigated using "*self-ionization*" produced under EI conditions by applying a large delay before the analytical scanning. In spite of the similarity of EI mass spectra of 1c and 1t, self-ionization mass spectra of the studied epimers now exhibit enhanced differences as reported in Fig. 5. Particularly, the presence of the diagnostic *m/z* 113 ions as well as the *m/z* 347, *m/z* 451, and *m/z* 469 adduct ions characterize 1t. However, under these self-ionization conditions, interestingly the *m/z* 217 ion is never stereospecific of 1c since it appears as a base peak for both isomers in contrast to those observed in previous CI–NH_3 mass spectra (Fig. 4).

4. Discussion

The use of methane and isobutane as gas phase reagents gives rise to production of several fragment ions due to competitive and consecutive dissociations from MH^+ containing a relative high internal energy as previously emphasized. Nevertheless, the stereospecific benzoic acid loss (i.e. formation of *m/z* 113) from the 1tH^+ epimer ions can be used for differentiation of the *cis*/*trans* geometry, even if this ion is characterized by a weak abundance due to consecutive decomposition into *m/z* 95 via water elimination (e.g. less 10% and 42.5% under CI–CH_4 and CI–iC_4H_{10} conditions, respectively). These results contrast with those characterizing the product ions in the electron impact mode (EI). Indeed, EI mass spectra of these epimers do not show large abundance changes according to the *cis*/*trans* geometry. Note that under these conditions the diagnostic *m/z* 113 ion of the 1t epimer is not detected.

4.1. Effect of the regioselectivity and stereospecificity from weakly excited molecular species prepared under ammonia chemical ionization conditions

Ready *cis* and *trans* distinction can be provided from analysis of the NH_3–CI mass spectra (Fig. 4).

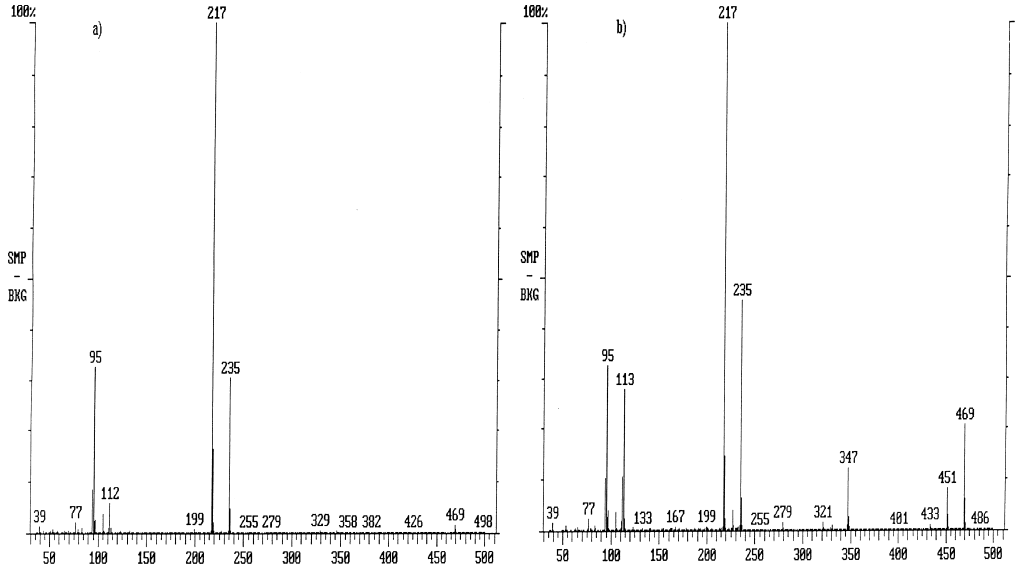

Fig. 5. Self-ionization mass spectra [for t_r = 80 ms as reaction time] of the isomeric (a) *cis* and (b) *trans* of the (4-hydroxy-4-methyl-cyclohexyl)-benzoate recorded according to the procedure described in Fig. 1(b).

Indeed, these differences in relative ion abundances appear for several ions such as the adduct MNH_4^+ ions (i.e. *m/z* 252) and the fragment ions (e.g. *m/z* 217, *m/z* 113, and *m/z* 95) as well as the containing nitrogen product *m/z* 234 and *m/z* 130 ions. These latter ions result from similar nucleophilic substitutions as the NH_3/NH_4^+ system. Particularly, the *trans* epimer exhibits more abundant MNH_4^+ ions, *m/z* 252 (as 60% of the base peak at *m/z* 113) than are observed from the *cis* epimer (i.e. less 10% of the base peak at *m/z* 217). Furthermore, it must be emphasized that in the ammonia CI mass spectrum of the *cis* 1c epimer, the reagent NH_4^+ and $N_2H_7^+$ ions are consumed, which is not entirely the case for the *trans* 1t epimer (Fig. 4).

The enhanced $\underline{1t}NH_4^+$ abundance as well as the presence of the survivor $NH_4^+/N_2H_7^+$ ions from the *trans* epimer relative to that observed from the *cis* epimer suggest [17] that $PA_{cis} > PA_{trans}$. The higher relative PA value of *cis* epimer can be attributed to the occurrence of hydrogen bonding which is possible within the twist (or/and boat) conformation, yielding stabilization of the attached proton. Such proton solvation is not conformationally possible for the *trans* epimer where no solvating group is nearby to the protonated groups [18]. Finally, observation of the MH^+ ions from both the epimers most likely indicates that $PA_{cis} > PA_{trans} > PA_{NH_3}$. This behavior is expected since PA of benzoate ester is known to be as slightly higher than that of ammonia [19].

4.1.1. Geometry of the different $\underline{1c}NH_4^+$ and $\underline{1t}NH_4^+$ forms due to the NH_4^+ solvation

Generally, nucleophilic (or/and basic) groups of these bifunctional compounds can be competitively linked for the NH_4^+ solvation. The relative stability of each possible product $\underline{1c}NH_4^+$ and $\underline{1t}NH_4^+$ form depends upon the difference between the relative proton affinities of the involved site and ammonia reagent. Hence, from the *trans* epimer, two solvated $\underline{a}NH_4^+$ and $\underline{b}NH_4^+$ forms can be considered because of the absence of conformational interaction between the functional groups (Scheme 3), which does not allow the $\underline{a}NH_4^+ \leftrightarrow \underline{b}NH_4^+$ interconversion. However, from the *cis* isomer where the basic sites are geometrically close, only the $\underline{c}NH_4^+$ form with hydrogen bonding should be considered as an intermediate form between the $\underline{a'}NH_4^+$ and $\underline{b'}NH_4^+$ forms within the twist (and/or boat) conformation. On the other hand, both the latter forms could also coexist (Scheme 4). The presence of the different solvated forms can be evidenced by

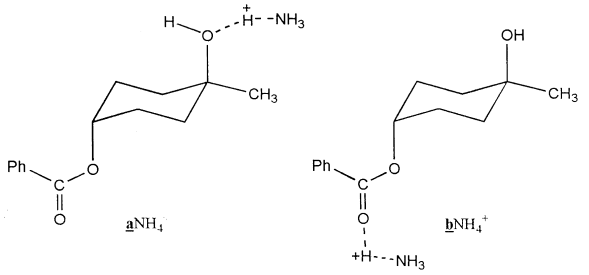

Scheme 3. Isomeric structures of the *trans* $\underline{1t}NH_4^+$ adduct ions (*m/z* 252).

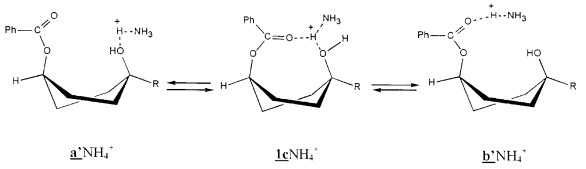

Scheme 4. Isomeric structures of the *cis* $\underline{1c}NH_4^+$ adduct ions (*m/z* 252).

analysis of consecutive decompositions via the assumed formation of the weakly stable MH^+ i.e. as $\underline{a}H^+$ and $\underline{b}H^+$ in addition to $\underline{c}H^+$, which are considered to fragment with a relative high rate constant into diagnostic fragment ions [20]. Actually for the $\underline{1t}$ epimer, consecutive dissociations of $\underline{a}NH_4^+$ leads to the loss of $\{H_2O + NH_3\}$ [i.e. formation of *m/z* 217, Eq. (1)-(ii)], in contrast with the $\underline{b}NH_4^+$ form that will lead to the $\{NH_3 + C_6H_5COOH\}$ neutral losses giving rise to the formation of the *m/z* 113 ions [Eq. (2)-(ii)]:

$$\underset{(m/z\ 252)}{\underline{a}NH_4^+} \xrightarrow[(-NH_3)]{(i)} \underset{(m/z\ 235)}{\underline{a}H^+} \xrightarrow[(-H_2O)]{(ii)} \underset{(m/z\ 217)}{[\underline{a}H\text{–}H_2O]^+} \quad (1)$$

$$\underset{(m/z\ 252)}{\underline{b}NH_4^+} \xrightarrow[(-NH_3)]{(i)} \underset{(m/z\ 235)}{\underline{b}H^+} \xrightarrow[(-C_6H_5COOH)]{(ii)} \underset{(m/z\ 113)}{[\underline{b}H\text{–}C_6H_5COOH]^+} \quad (2)$$

The ammonia CI mass spectrum (Fig. 4) mainly displays the peak at *m/z* 113, which emerges as a base peak among the various fragment ions, in contrast to the less complex pathway leading to *m/z* 217 (20% of base peak). This result indicates that the $\underline{b}NH_4^+$ form (NH_4^+ being solvated by the benzoate group) plays the main role in the dissociation orientation of the $\underline{1t}NH_4^+$ ion. This contrasts with dissociation of the adduct $\underline{1c}NH_4^+$ ion as shown in CI/NH_3 mass spectrum of $\underline{1}$ which displays only the consecutive losses of the $\{NH_3 + H_2O\}$ neutrals (i.e. favored formation of the *m/z* 217 ions).

4.1.2. Why is the NH_4^+ solvation regioselective at the benzoate site for the trans $\underline{1t}$ epimer?

As previously emphasized, both the nucleophilic sites of $\underline{1t}$ may independently solvate ammonium, which is due to the exothermicity of such solvation reaction [21]. However, very likely kinetic effects can hinder the NH_3 approach to the reactive site (i.e. steric effect as well as polarisability of nucleophilic groups) [20] resulting into a lowering of the bimolecular rate constant. In order to appreciate whether the $\underline{a}NH_4^+$ or $\underline{b}NH_4^+$ form is favored, abundant fragment ions obtained (1) from spontaneous decompositions of adduct ions (i.e. displayed in the CI–NH_3 mass spectrum) and (2) from CID of the survivor adduct $\underline{1t}NH_4^+$ ions, are compared [20] (Table 2).

This discussion is based upon the rule [22] that implies that from bifunctional protonated molecules, the leaving group corresponds to that which loses a neutral having the lower PA value. Thus, it is expected that the water elimination from decomposing $\underline{a}H^+$ ions [Eq. (1)-(ii)] must occur with a higher rate constant than that of the benzoic acid elimination from the $\underline{b}H^+$ ions because of PA values [19] of the lost neutrals i.e. $PA_{H_2O} = 697$ kJ mol^{-1} and $PA_{C_6H_5COOH} = 829$ kJ mol^{-1}. However, this anticipation is in contrast to that observed in ammonia CI mass spectrum (Fig. 4), which displays *m/z* 217 (25%

Table 2
Different product ions displayed in low energy CID spectra of the epimeric $\underline{1c}NH_4^+$ and $\underline{1t}NH_4^+$ adduct ions (*m/z* 252) prepared under CI/NH_3 conditions (ion abundances are relative to the base peak as 100% and in brackets, the ion abundances relative to the base peak displayed in the NH_3–CI mass spectra).

	m/z 95	*m/z* 113	*m/z* 130	*m/z* 140	*m/z* 217	*m/z* 234	*m/z* 235	*m/z* 252
$\underline{1c}NH_4^+$	4.4 (8.2)	. . .	. . .	. . .	100 (100)	11 (1)	. . .	20 (4.4)
$\underline{1t}NH_4^+$	44 (35.6)	100 (100)	35 (40)	2.2 (4.4)	4.4 (22)	. . .	6.5 (14.9)	65 (61.8)

of base peak) and *m/z* 113 as base peak, corresponding to the loss of water from $\underline{a}H^+$ and benzoic acid from $\underline{b}H^+$, respectively.

This result suggests that in the ion source, the $\underline{b}H^+$ form should favorably be generated relative to the $\underline{a}H^+$ isomeric form from the *trans* epimer. This may be expected by considering that the PA_{NH_3} value is higher than $PA_{(\text{tertiary alcohol})}$ (*vide supra*) and reversibly for the ester. In the case of $\underline{1c}$, the previous expected behavior is consistent with the ammonia CI mass spectrum (Fig. 4) since the loss of benzoic acid is entirely hindered and loss of water becomes the major decomposing pathway. This is explained by the existence of a particular conformation of ions where the ionizing proton can migrate from a nucleophilic site to the second one. The envisaged $\underline{c}NH_4^+$ forms can yield the intermediate $\underline{c}H^+$ ions which specifically dissociate into *m/z* 217 by loss of water [Eq. (3)] according to a higher unimolecular rate constant relative to the benzoic acid loss. On the other hand, the importance of consecutive decompositions of the stereospecific *m/z* 113 ion from $\underline{1t}$ and the diagnostic *m/z* 217 ion (from $\underline{1c}$) into the common *m/z* 95 ions (i.e. $C_7H_{11}^+$) by losses of H_2O and C_6H_5COOH, respectively, is consistent with the previously used rule. Indeed, the elimination of water from *m/z* 113 is particularly enhanced in comparison of that of benzoic acid which is much weaker from $\underline{1c}NH_4^+$

$$\underset{(m/z\ 252)}{\underline{1c}NH_4^+} \xrightarrow[(-NH_3)]{\text{(i)}} \underset{(m/z\ 235)}{\underline{1c}H^+} \begin{cases} \xrightarrow{\text{(ii)}} [\underline{1c}H\text{–}H_2O]^+ + H_2O \quad (m/z\ 217) \\ \xrightarrow{\text{(iii)}} [\underline{1c}H\text{–}C_6H_5COOH]^+ + C_6H_5COOH \quad (m/z\ 113) \end{cases} \tag{3}$$

Thus at this point, it is difficult to determine from $\underline{1t}$ why the intermediate $\underline{a}H^+$ ions are weakly produced: either its formation is too endothermic from $\underline{a}NH_4^+$ [Eq. (1)-(i)] or production of the adduct $\underline{a}NH_4^+$ ions is reduced or kinetically and thermochemically unfavored. However, based upon the relative stability of the $\underline{a}NH_4^+$ ions toward the dissociation into either $\{\underline{1t} + NH_4^+\}$ or $\{\underline{a}H^+ + NH_3\}$, a possible rationalization may be proposed. Indeed, from investigations on protonated clusters [23], it has been shown that the more the proton affinity of neutrals, which solvate the protons, are similar, the more the cluster stability is enhanced. Applied to the study of the $\underline{a}NH_4^+$ and $\underline{b}NH_4^+$ systems, it is possible qualitatively to appreciate whether the $\underline{a}NH_4^+$ or $\underline{b}NH_4^+$ form is the most stable.

Consider that the (1) $PA_{[tC_6H_{10}(CH_3)(OH)]}$ and $PA_{[C_6H_5CO_2C_6H_{11}]}$ values are estimated as 820.5 and 889.5 kJ mol^{-1}, respectively (see the Appendix) [23] and (2) PA_{NH_3} = 857 kJ mol^{-1}. Then, the $[PA_{\text{solvating site}}\text{–}PA_{NH_3}]$ difference is larger from the tertiary hydroxyl site than that from the benzoate site, consequently it may be expected that $\underline{a}NH_4^+$ is less stable than $\underline{b}NH_4^+$. The former decomposes into NH_4^+ rather than into $\underline{a}H^+$ because $PA_{NH_3} > PA_{ROH}$. Thus, the $\underline{a}NH_4^+$ form participates in a much weaker contribution than $\underline{b}NH_4^+$ in the dissociated adduct $\underline{1t}NH_4^+$ ions. In order to confirm the solvation site, the survivor $\underline{1t}NH_4^+$ and $\underline{1c}NH_4^+$ ions characterized by a longer lifetime have been investigated under low energy collision conditions after ion selection (Table 2).

Table 3
Different product ions displayed in CID spectra of the epimeric $\underline{1c}H^+$ and $\underline{1t}H^+$ ions (*m/z* 235) prepared under CI/NH_3 conditions (ion abundances are relative to the *m/z* 235 parent ion) and in brackets are reported the relative ion abundances of product ions formed from CID of the epimeric *m/z* 235 ions generated by self-ionization

	m/z 95	*m/z* 113	*m/z* 130	*m/z* 140	*m/z* 217	*m/z* 234	*m/z* 235	*m/z* 252
$\underline{1c}H^+$	. . .	. . .	. . .	. . .	76.5 (100)	24	100 (55)	32
$\underline{1t}H^+$	. . . (8)	61 (51)	24	4.5	10.5 (39)	4.5	100 (100)	45

The CID spectra of the epimeric adduct *m/z* 252 ions (Table 2) are similar in trend to the CI mass spectra and only a few changes in ion abundance can be observed. In particular, the CID spectrum of $\underline{1t}NH_4^+$ displays a fragment *m/z* 217 ion (diagnostic to the $\underline{a}NH_4^+$ form) in a lower abundance relative to its precursor *m/z* 252 ions (i.e. approximately 0.06, Table 2) compared to the [*m/z* 217]/[*m/z* 252] ratio measured as 0.33 from the CI mass spectrum of $\underline{1t}$ (Fig. 4). This indicates that contribution of the $\underline{a}NH_4^+$ form relative to that of the $\underline{b}NH_4^+$ form in the survivor adduct $\underline{1t}NH_4^+$ ions (submitted to resonant excitation) is decreased compared to its contribution in the adduct ions, which spontaneously decompose as shown from the CI mass spectrum. This confirms our previous assumption, which considers that the $\underline{a}NH_4^+$ form is (1) produced under a lower yield than it is for the $\underline{b}NH_4^+$ form and (2) less stable than its isomeric form.

4.1.3. Site involved by ion–molecule reactions other than proton exchange

Under positive ion chemical ionization, the nucleophilic substitution reaction induced by the NH_3/NH_4^+ system is generally favored when protonation is an endothermic process [24]. Then, competition in favor of the nucleophilic substitution pathway gives rise to formation of the substituted M_SH^+ ion (e.g. $[MNH_4–H_2O]^+$ from alcohols) [25] in high abundances relatively to those of the MH^+ ions. This behavior implies that (1) the neutral nucleophilic NH_3 reagent have a basicity slightly higher than that of the substrate and (2) the adduct MNH_4^+ ions are formed as stable precursor species of such ion–molecule reactions.

In addition to the previously observed differences from dissociation in CI mass spectra, two stereospecific ions, $[M + NH_4–C_6H_5COOH]^+$ (*m/z* 130) and $[M + NH_4–H_2O]^+$ (*m/z* 234), are observed from the *trans* epimer and the *cis* epimer, respectively. These ions may be considered as similar to "like substituted ions." Formation of the $[M + NH_4–C_6H_5COOH]^+$ ion (*m/z* 130) rather than $[M + NH_4–H_2O]^+$ (*m/z* 234) from the *trans* epimer confirms that the favorable ammonium solvation site (as well as the protonation site) is located at the ester position. Note that from the *cis* epimer, formation of the weak $[M + NH_4–H_2O]^+$ ion is significantly enhanced relative to that observed from the *trans* $\underline{1t}$ epimer. A similar conclusion can be provided from CID spectra of the epimeric MNH_4^+ ions (Table 2) as well as from those of the MH^+ ions (Table 3). Especially, from the CID spectra of $\underline{1c}H^+$, the substituted *m/z* 234 ion appears significantly enhanced compared to that produced from the selected $\underline{1t}H^+$ precursor ions. This latter prefers to yield formation of the *m/z* 130, $[C_7H_{11}, NH_3]^+$ and *m/z* 140 $[C_6H_5COOH, NH_4]^+$ ions (Table 3) produced very likely through ion–molecule reactions induced by presence of ammonia in the ion trap cell.

Furthermore, in CI mass spectrum of the $\underline{1t}$ epimer, production of $\underline{1t}H^+$ is strongly favored rather than $[\underline{1t}NH_4–H_2O]^+$. The formation of substituted $[\underline{1c}NH_4–H_2O]^+$ ions from the *cis* epimer is somewhat unexpected. The reverse behavior should be observed since $PA_{cis} > PA_{trans}$. This peculiarity may be rationalized by considering that likely (2) the adduct ions and more favorably the MH^+ ions react with NH_3 via the S_N2 process and (2) this reaction is internally catalyzed by the proton chelated by both the hydroxyl and benzoate ester sites yielding activation towards the NH_3 neutral approach [Scheme 5(a)]. Such activation results in an enhanced formation of the $[\underline{1}NH_4–$

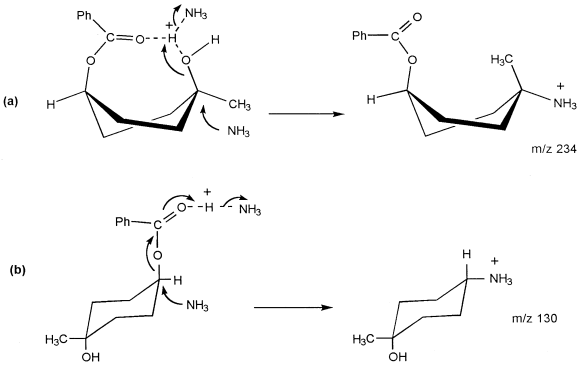

Scheme 5. S_N2 processes occurring from (a) the *cis* adduct $\underline{1c}NH_4^+$ ion and (b) the *trans* adduct $\underline{1t}NH_4^+$ ions.

$H_2O]^+$ ions (*m/z* 234) related to the loss of the better leaving group in gas phase from the *cis* form [Scheme 5(a)]. On the other hand, stereospecific formation of the *m/z* 130 ions from the *trans* epimer site likely may be caused by a similar internal catalysis by location of proton at the benzoate group which actives the S_N2 process [Scheme 5(b)]. Investigation of both the (a) and (b) hypothetical processes will be confirmed by additional experiments in progress which will be published elsewhere.

Complementary, the ND_3–CI mass spectra of the <u>1c</u> and <u>1t</u> stereoisomers show that the peaks at *m/z* 130 and *m/z* 234 are, respectively, shifted by 4 Th at *m/z* 134 and *m/z* 238 (instead of *m/z* 237 as expected for a conventional nucleophilic substitution process) [26]. This experiment is carried out under higher reagent gas pressure in order to avoid adduct ion dissociation into the MH^+ ions without hindering the ion–molecule reactions. The fact that the *m/z* 234 ions are shifted at *m/z* 238 and not at *m/z* 237 indicates that the structure of this ion differs from the expected covalent structure for the substituted ions as those obtained by these processes [25]. This *m/z* ratio shift suggests that the nucleophilic substitution pathway plays a minor role and as an alternative, another mechanism must be considered. This behavior is not surprising because of a steric hindrance at the electrophilic carbone site (i.e. activated tertiary alcohol) which prevents the direct nucleophilic substitution reaction. On the other hand, this phenomena favors formation of an ion/neutral

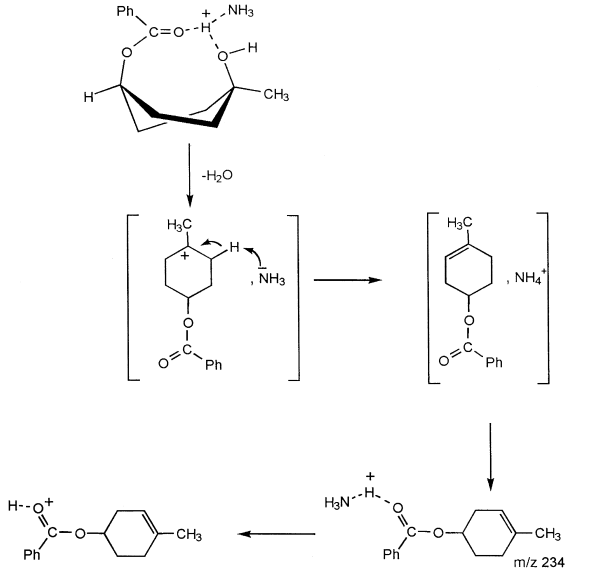

Scheme 6. Formation of the *m/z* 234 ion *via* isomerization into an ion/neutral complex prior to dissociation.

complex [27] {i.e. $[R^+, NH_3]$ or/and $[(R–H), NH_4^+]$} (Scheme 6).

Moreover, formation of the $[M + NH_4–C_6H_5COOH]^+$ ion (*m/z* 130) from the *trans* epimer can be explained by two different processes: (1) the nucleophilic substitution regioselectively occurs at benzoate site activated by presence of proton as catalyst [Scheme 7(a)] and/or (2) elimination of the benzoic acid neutral is carried out by a stepwise process occurring *via* an ion/neutral complex formation leading to in competition mainly, $[M + NH_4–C_6H_5COOH]^+$ (*m/z* 130) and in a lower abundance, $[C_6H_5COOH + NH_4]^+$ (*m/z* 140). Very likely, the larger PA difference which exists between benzoic acid and NH_3 in comparison with tertiary cyclohexanol and NH_3 (*vide supra*), explains why $C_6H_{10}(CH_3)OH_2^+$ (or $[M + NH_4–C_6H_5COOH]^+$) is more stable than $[C_6H_5COOH + NH_4]^+$ ion by considering that both the ions are hydrogen bonded forms [22] under the CID conditions.

Nevertheless, this justification does not allow enlightenment on the origin of the ambiguous *m/z* 130 ion which can be generated either by a S_N2 and/or S_Ni process occurring at the benzoate site of MH^+ or by

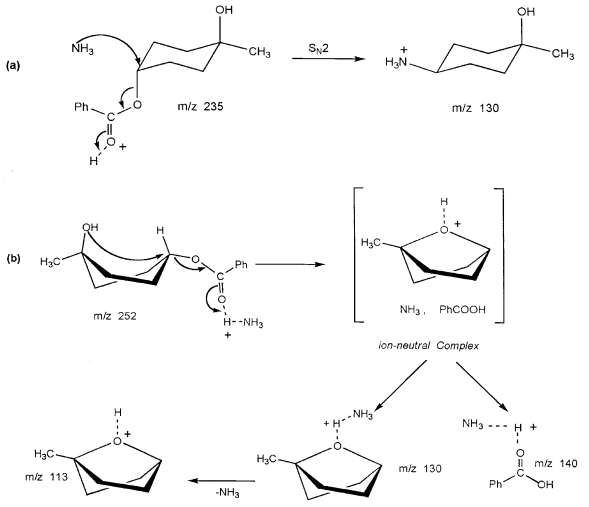

Scheme 7. Formation of the *m/z* 130 ion generated from (a) a S_N2 reaction or *via* (b) an isomerization into ion/neutral complex.

NH_3 solvation of the protonated fragment ether (*m/z* 113) yielding a proton-bounded adduct ion (*m/z* 130) (Scheme 7). Note that from high pressure source of conventional tandem mass spectrometer (i.e. triple quadrupole and reversed geometry sector instruments) [12], similar fragment *m/z* 217 and *m/z* 113 ions are observed under collision conditions. However, both the *m/z* 130 and *m/z* 140 ions related to ion–molecule reactions were not produced in significant abundance [12].

4.2. Role of EI fragment ions on the formation of the protonated molecules and adduct ions related to the cis *and* trans *stereochemistry under self-ionization conditions*

4.2.1. Contribution of EI fragment ions for giving proton to neutral yielding MH^+ with larger internal energy distributions in comparison to that observed under CI/NH_3 conditions

To achieve the *self-ionization* conditions, the EI mass spectra of epimers (Fig. 5) have been recorded by using 80 ms as a reaction period to allow a series of ion/molecule reactions induced by the EI fragment ions on the neutral. This delay time was applied prior to application of the full analytical scan and without using the segmentation steps. The *self-ionization* mass spectra of epimers do not display fragment ions originated from the direct EI processes. Alternatively, this means that all EI fragment ions mainly react through exothermic pathway with epimeric neutrals to be entirely consumed. This gives rise to formation of (1) the epimeric MH^+ ions (*m/z* 235), (2) the fragment ions of MH^+ from 1c such as the *m/z* 95, and *m/z* 217 ions and from 1t, *m/z* 95, *m/z* 113, and, *m/z* 217, and (3) various adduct ions and proton-bounded homodimers specifically for the *trans* epimer.

Observation of the consecutive fragment *m/z* 95 ion produced from the $1cH^+$ ion indicates that certain precursor ions contained more internal energy than occurs in CI–NH_3 since this fragment ion is not produced in high yield especially from 1c. On the other hand, detection of the dimeric species at least for 1t, suggests that a fraction of the produced $1tH^+$ ions from *self-ionization* conditions contains weaker internal energy than in CI/NH_3. Indeed, the latter CI conditions do not allow production of dimeric M_2H^+ ions (*m/z* 469) even at longer delay prior to the analytical scan (Fig. 6). However, the fragment *m/z* 130, *m/z* 113, and *m/z* 95 ion abundances, in CI–NH_3, decreases in favor to that of the *m/z* 217 ion, which is increased. This reflects an unexpected enhancement of the water loss from 1t. Such a behavior can be explained by assuming that the EI fragment ions at low *m/z* ratios react with the 1t neutral by possible protonation at the OH site. Indeed, its PA value is very likely close to those of the alkene neutral (related to the *m/z* 95 ion) and the ether neutral (related to *m/z* 113) as previously determined. Thus, the product MH^+ ions in CI–NH_3 after a delay time decompose through the water loss according to a higher rate constant than occurs with the benzoic acid loss.

Thus, under *self-ionization* conditions [13], these observations suggest that the parent ions are produced with a broad internal energy distribution. This is related to the diversity of the EI fragment ions implicated during production of the even-electron quasimolecular species after the delay time for inducing self-ionization processes.

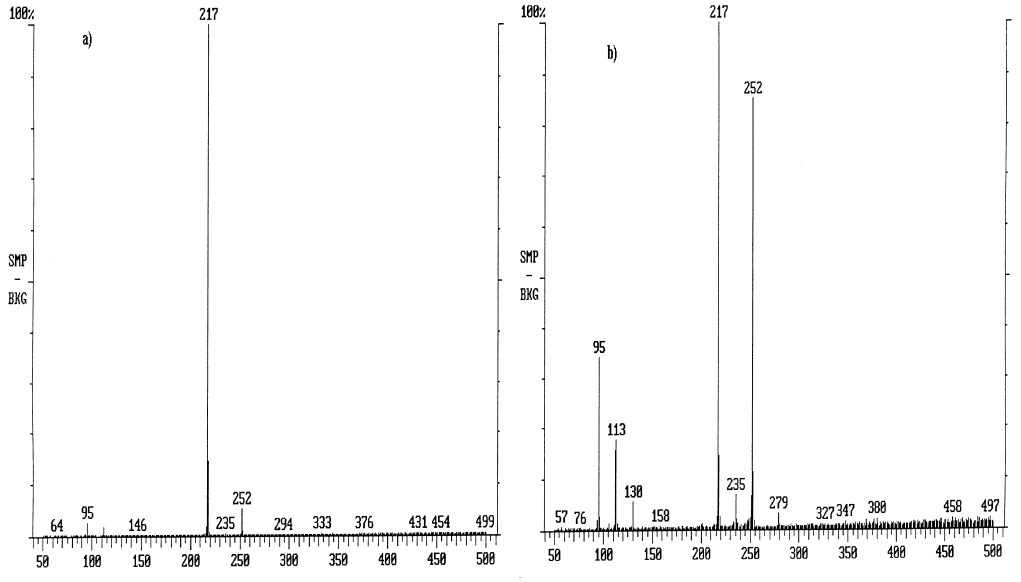

Fig. 6. CI ammonia mass spectra (within a reaction time of 80 ms) of the isomeric (a) *cis* and (b) *trans* of the (4-hydroxy-4-methyl-cyclohexyl)-benzoate recorded according to the procedure described in Fig. 1(a).

4.2.2. Comparative reactivity of the EI fragment m/z 43 and m/z 123 ions towards epimers

In order to enlighten the mechanisms of the various ion–molecule reactions, selective isolation of the EI fragment ions [28] has been applied to provide particular reagent ions able to induce bimolecular processes. Especially, the reactivity of the reagent *m/z* 43 and *m/z* 123 ions, respectively, considered as protonated ketene and benzoic acid forms, have been investigated according to the time range (t_r) chosen for producing bimolecular processes. These ions can be generated from exothermic proton transfer by considering that $PA_{(M)}$ is estimated to be close to $PA_{(NH_3)}$ (i.e. 854 kJ mol^{-1}) and for the reagent neutrals [19], i.e. $PA_{(CH_2{=}C{=}O)}$ = 657 kJ mol^{-1} and $PA_{(C_6H_5COOH)}$ = 829 kJ mol^{-1}. Indeed, the exothermicity values of proton transfer approximatively are of 200 and 25 kJ mol^{-1} by using *m/z* 43 and *m/z* 123 as reagent ions, respectively. Thus, the former EI fragment ion is able to protonate the epimeric neutrals to give rise to formation of the $\underline{1c}H^+$ and $\underline{1t}H^+$ ions (i.e. *m/z* 235 ions) containing large internal energy and thus allowing decompositions with a high rate constants.

First, as this delay is raised, the selected EI reagent ions are entirely consumed by reactions leading to the MH^+ ions (*m/z* 235). The abundance of these protonated molecules reaches an optimum value at t_r = 20 ms as a reaction time and slightly decreases at higher values. This behavior contrasts those of the dimeric *m/z* 469 ion and the fragment *m/z* 217 ion, which increase as t_r increases. The increase of the latter ion is unexpected since it should disappear as occurs for the fragment *m/z* 113 and *m/z* 95 ions (Figs. 7 and 8). This difference in abundance behavior for the *trans* epimer can be rationalized by the following considerations. (1) At a longer reaction time, the product *m/z* 95 and *m/z* 113 ions may regenerate the MH^+ precursor exothermically at benzoate site ($\underline{b}H^+$ form) as well as at hydroxyl site ($\underline{a}H^+$ form). Indeed, most likely the proton affinity of the studied substrate is higher than that of the methylcyclohexene and the methylcyclohexene ether related to the protonated *m/z* 95 form and the protonated *m/z* 113 ions, respectively (Scheme 7). (2) The product *m/z* 217 ions occur from the decomposition of the protonated MH^+ ions having high internal energy. This confirms that from $\underline{1t}H^+$, formation of the isomeric $\underline{a}H^+$ form takes place

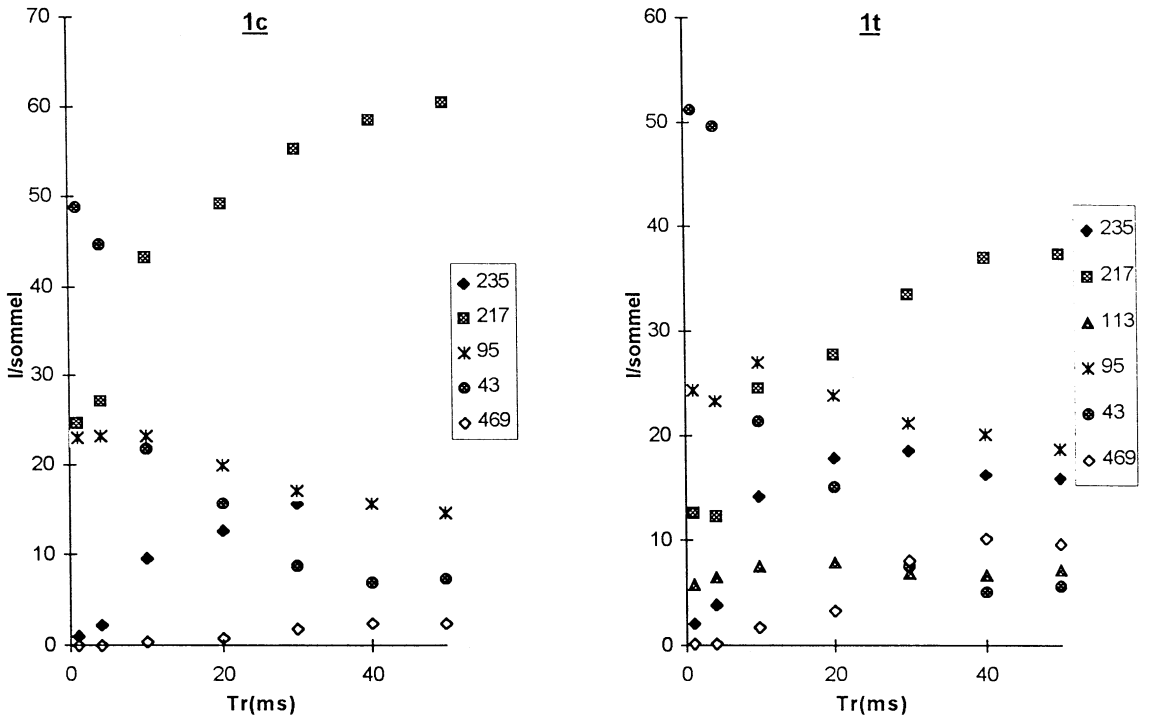

Fig. 7. Variation of relative abundance of the product ions from ion–molecule reactions induced by the *m/z* 43 reagent ion upon the reaction time with the isomeric (a) *cis* and (b) *trans* isomers of the (4-hydroxy-4-methyl-cyclohexyl)-benzoate.

(*vide supra*). (3) Reversibly, the stability of the *m/z* 217 ions toward proton transfer to the M neutral is consistent with the proposed structure for the survivor *m/z* 217 ion (i.e. protonated benzoate form yielding weakly efficient proton transfer to M) as shown in Scheme 6. Thus, *m/z* 217 must be accumulated as the t_r value is raised. (4) Finally, formation of the hydrogen-bonded homodimer is enhanced at higher reaction time. The favorable observation of dimer from the 1t epimer indicates that the protonated $\underline{1t}H^+$ molecule preserves its initial *trans* geometry.

Furthermore, Figs. 7 and 8 show that, independent of the selected *m/z* 43 or *m/z* 123 reagent ions, a similar trend characterizes the abundance progression of the product ions upon the reaction time. The ion abundances are enhanced from the 1t epimer showing a larger reactivity toward dissociation as well as dimerization in comparison with that occurring from the 1c epimer. However, after a reaction time of a few milliseconds, induced by the protonated *m/z* 43 ketene as reagent, ion–molecule reactions are especially increased, particularly the consecutive fragmentations yielding the *m/z* 95 ions (#20% of TIC) from both the epimers relatively to that observed (i.e. less than 5% of the TIC) by using the protonated *m/z* 123 benzoic acid as reagent. From the latter self-ionization conditions, the strong decrease of the *m/z* 95 abundance indicates that the product MH^+ ions have less internal energy. This reflects a larger exothermicity achieved by using the *m/z* 43 reagent relative to that which occurs with the *m/z* 123 reagent for MH^+ formation due to their relative PA (*vide supra*).

Based upon these considerations, it can be concluded that during the MH^+ formation, the internal energy is preserved as shown by the increased consecutive dissociation rate constants with protonated ketene reagent. Then, it is not entirely relaxed as expected through multiple collisions with helium as buffer gas which thermalizes only the kinetic energy of the ions [29] in the ion trap cell; however neutral

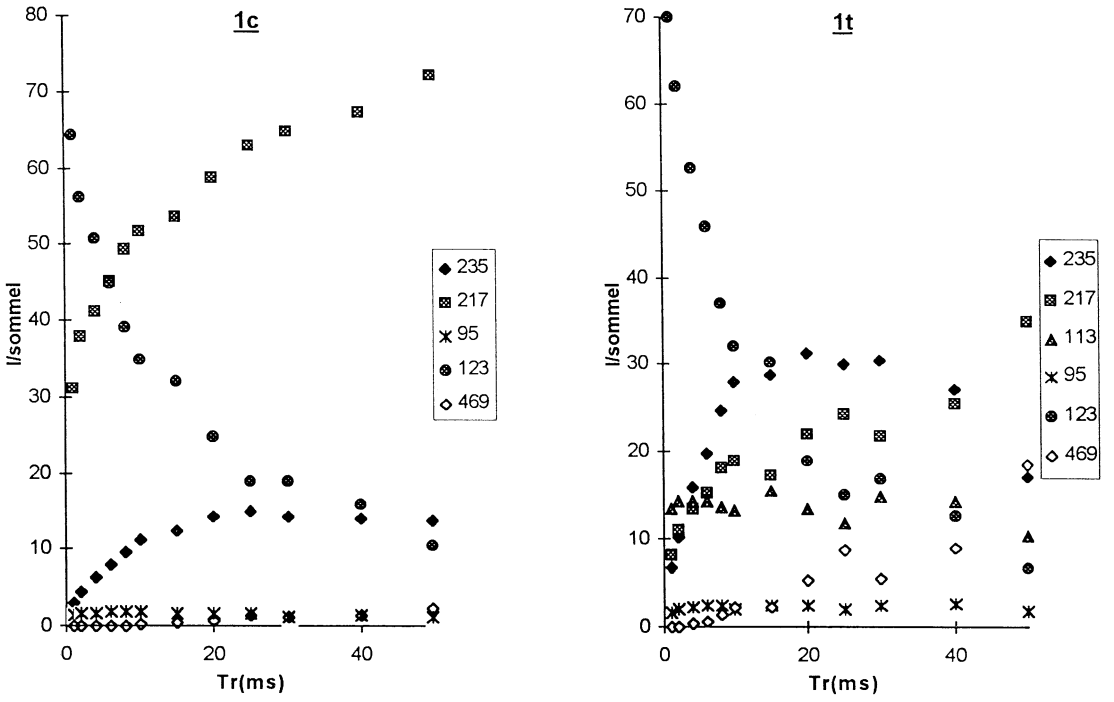

Fig. 8. Variation of relative abundance of the product ions from ion–molecule reactions induced by the *m/z* 123 reagent ion upon the reaction time with the isomeric (a) *cis* and (b) *trans* isomers of the (4-hydroxy-4-methyl-cyclohexyl)-benzoate.

epimers being in excess, collisions yield long-life ion–dipole complexes. These may allow a partial randomization of the internal energy over the different oscillators providing a partial vibrational energy relaxation. Alternatively, this means that the internal energy distribution, likely broad as demonstrated previously, is shifted towards lower energy range according to the exothermicity of the protonation process.

Note that the absence of *m/z* 113, in spite of the broad internal energy distribution carried out by the $\underline{1c}H^+$ ions, gives evidence of the occurrence of an anchimeric assistance for the benzoic acid loss observed from $\underline{1t}H^+$. In the latter parent ion, the protonation takes place competitively at the benzoate and hydroxyl sites as previously shown. In the case of the *cis* epimer, both the nucleophilic sites can be reversibly protonated however, such an anchimeric assistance cannot occur and only water is lost rather than benzoic acid.

4.2.3. Unspecific protonation site under self-ionization conditions

For these molecules which contain two nucleophilic functions, protonation should occur at site having the higher gas-phase basicity than the reagent ions as previously emphasized. Hence, from the resonant CID spectrum of the protonated *trans* epimer prepared in the self-ionization conditions (Table 3), the elimination of benzoic acid yielding $[MH–C_6H_5COOH]^+$ (*m/z* 113, as for 51% of the *m/z* 235 base peak) is observed and should be stereospecifically observed if protonation takes place regioselectively at the benzoate site. However, the presence of an intense *m/z* 217 ion (39% of parent *m/z* 235 ion) is detected, which reflects that protonation also competitively occurring at the OH site when protonated molecules are prepared in self-ionization. Furthermore, the situation is more dramatic in the self-ionization mass spectrum of $\underline{1t}$ since its base peak is not related to *m/z* 113 but it is at *m/z* 217, thus the

$[MH–H_2O]^+$ ion appears to be formed by the main process (Fig. 5).

This particular behavior indicates that protonation takes place in competition at both benzoate and hydroxyl sites in contrast with that observed under CI ammonia conditions at low delay time by proton transfer from NH_4^+ (Fig. 6). This difference in behavior is rationalized by considering the relative lower PA value of EI reagent ions (e.g. $PA_{(CH_2=C=O)}$ = 657 kJ mol^{-1} and $PA_{(C_6H_5COOH)}$ = 829 kJ mol^{-1}) [19] than that of the tertiary alcohol and the benzoate group. Thus, under self-ionization conditions as well as at longer delay time in CI–NH_3 both the isomeric $\underline{a}H^+$ and $\underline{b}H^+$ nonconvertible forms of the $\underline{1t}H^+$ ions must be considered (Fig. 6). However, the isomeric $\underline{a}H^+$ form must decompose according to a higher rate constant than from the $\underline{b}H^+$ form since the lost neutral corresponds to the group having the lower PA value [22] and the water elimination is reinforced in comparison with that of benzoic acid. However, this orientation does not affect the *cis*/*trans* differentiation since the *m/z* 113 ion remains stereospecific of the *trans* geometry. The limited formation of $[MH–C_6H_5COOH]^+$ (*m/z* 113, displayed in Fig. 4) must be compared to that observed in ammonia CI where *m/z* 113 corresponds to the base peak, whereas the abundance of the $[MH–H_2O]^+$ ion is approximately 20% of that of the fragment *m/z* 113 ion (Fig. 6), which is reversed after a longer time of reaction (i.e. 80 ms as delay time).

Concerning the *cis* epimer, the possible interaction between both the neighbored functional groups allows the reversible isomerisation of $\underline{a}'H^+$ into the $\underline{b}'H^+$ forms (or reversibly). These isomeric forms are able to yield competitive dissociations *via* the intermediate $\underline{c}H^+$ form (Scheme 4). This is confirmed by large abundance of $[MH–H_2O]^+$ (*m/z* 217 as base peak) corresponding to an endothermic proton transfer from protonated benzoate site to the hydroxyl function inducing the loss of the group characterized by the lower PA value. This means that prior to decomposition, the $\underline{b}'H^+$ form is submitted to a total isomerisation, in spite of its endothermic character and that the decomposing $\underline{1c}H^+$ ions are completely evacuated within the $\underline{a}'H^+$ form. This result is an additional illustration of the role played by the ion isomerisation prior to any dissociation.

Formation of various dimeric forms (or decomposed ones) such as the cluster $[M + 113]^+$, $[M + 217]^+$, and $[2M + H]^+$ ions (i.e. *m/z* 347; *m/z* 451; and *m/z* 469, respectively) specifically are detected for $\underline{1t}$. The two former are generated by ion–molecule reactions induced by the fragment *m/z* 217 and *m/z* 113 ions. The *m/z* 469 ion appears with a lower abundance from the $\underline{1c}$ epimer than those observed from $\underline{1t}$. Respective investigation of the formation mechanisms of these various adduct ions (as hydrogen-bonded forms or/and covalent adduct species) as well as their respective structures are in progress and, at this moment the stereospecific presence of these signals is only useful for distinguishing diastereoisomers under self-ionization conditions.

5. Conclusion

This study demonstrates the analytical potential of ion trap mass spectrometer for distinguishing diastereoisomers such as *cis*/*trans* hydroxy-benzoate methyl-cyclohexyls. First, independent of properties of the reagent gas (i.e. its PA as well as its nucleophilic character) used for performing CI mass spectra, the epimer stereochemistry is determined without ambiguity. That is achieved from the *trans* epimer by comparison of the relative abundances of (1) MH^+ and MNH_4^+ observed in significant abundances and (2) fragment ions since from decompositions of MH^+ ions, with high rate constants, the loss of benzoate acid is stereospecific and takes place *via* anchimeric assistance.

This behavior contrasts with the common water elimination strongly reinforced for the *cis* epimer, especially under NH_3–CI conditions (>70% of TIC). From the *trans* epimer where the functional groups are not neighboring, such a specific benzoic acid loss gives evidence of the stereospecific protonation at the benzoate group rather than at the hydroxyl site, in spite of the coexistence of both solvated MNH_4^+ forms. Water loss from the unstable protonated hydroxyl form does not require intramolecular assis-

tance because in the gas phase the activated $-OH_2^+$ group can be considered as a notable leaving group in comparison with the protonated benzoate, which is less labile. On the other hand, for the *cis* epimer, this orientation is reflected by absence of $[M + NH_4–C_6H_5COOH]^+$ because the ionizing proton at the benzoate site is more easily transferred to the OH site for inducing water loss rather than yielding direct loss of benzoic acid. As expected, this orientation is related to the relative PA values of ammonia and of the implied nucleophilic group of the studied substrate.

Similar conclusions are provided by using the quadrupole and sector mass spectrometers. However, CI mass spectra which are recorded by using an ion trap mass spectrometer, displayed: (1) enhancement of the *cis*/*trans* geometry differentiation and (2) the appearance of substituted $[M + NH_4–C_6H_5COOH]^+$ ions and solvated $[NH_3, C_6H_5COOH_2^+]$ adduct ions from the *cis* and *trans* epimers, respectively. This takes place in spite of the low ammonia pressure employed for performing chemical ionization, which reflects the role played by the larger residence time in the trap cell on the product ions resulting from reactions induced by reagent ions with epimeric neutrals.

On the other hand, CID spectra of the selected MH^+ ions present a special behavior since both the dissociative and solvating processes occur. This is demonstrated by presence of the diagnostic $[MH–H_2O]^+$ and $[MH–C_6H_5COOH]^+$ ions in addition to their corresponding solvated NH_3 forms such as $[MH–H_2O + NH_3]^+$ and $[MH–C_6H_5COOH + NH_3]^+$, respectively. These ions result from stereospecific ion–molecule reactions: (1) between ammonia and selected MH^+ ions (and/or product adduct MNH_4^+ ions) from the *cis* epimer *via* formation of ion–dipole complex as a hydrogen-bonded form for the former product ion, and (2) between ammonia and the fragment $[MH–C_6H_5COOH]^+$ ions for the latter, from the *trans* epimer. A similar trend is characterized in the CID spectra of the adduct MNH_4^+ ions in spite of the observation of less abundant fragmentations. Observation of such ion–molecule reactions from experiments performed in the ion trap cell indicates that many of reactive ions contain very low kinetic energy, allowing bimolecular processes. Furthermore, they are produced regardless of the internal energy transferred to the ions during the ion excitation step; this internal energy is not relaxed by the multiple collisions occurring with helium. This suggests that to be reactive, one portion of the fragment and precursor ions must be focused at the trap center where the kinetic energy is the lowest as possible.

Finally, by using a long delay time between the electron impact ionization step and the application of the analytical scan, mainly *self-ionization* processes induced by all the EI fragment ions involve a large variety of more or less exothermic proton transfers. It results in a complete fingerprint change of the identical EI mass spectra of epimers. Then, within a certain delay time, these spectra become characteristic of the *cis*/*trans* geometry according to the same diagnostic ions as those observed under CI conditions. Furthermore, stereospecific processes yield adduct ions observed at higher *m/z* range than the quasimolecular ions. These dimeric forms constituted by fragment ions and neutral epimer are only observed from the *trans* epimer in spite of nonspecific protonations. Actually, from *trans* epimer the hydroxyl protonation takes place as shown by the presence of $[MH–H_2O]^+$ related to the base peak in addition to the *cis* epimers. Nevertheless, the stereochemistry differentiation based upon the formation of the $[MH–C_6H_5COOH]^+$ ion is possible either directly or from the particular appearance of the adduct $\{M + [MH–C_6H_5COOH]\}^+$ ion. This latter adduct ion was not observed from the CI experiments.

It is necessary to emphasize that the use of selected EI fragment ions such as the $C_6H_5COOH_2^+$ and CH_3CO^+ ions allows the formation of protonated molecules, respectively, carrying out low and large internal energies due to the proton transfer exothermicity as shown from the abundance of the consecutive fragment $C_7H_{11}^+$ ions. Indirectly, this gives evidence on the preservation of the added internal energy and the absence of its increase upon multiple collisions with helium. This phenomenon does not limit the secondary ion–molecule reactions, induced by $[MH–C_6H_5COOH]^+$ from the *trans* epimer, giving

rise to formation of the adduct ion as should be expected. Instead, the product $[MH–H_2O]^+$ ions from the *cis* and *trans* epimers do not yield secondary bimolecular processes, which shows the role played by the chemical nature of the reactive ions in the gas phase.

Appendix: estimates of thermochemical values

Considering that no interaction takes place between both the functional hydroxyl and benzoate groups (i.e. for *trans* hydroxyl benzoate isomer), the proton affinity (PA) values of the tertiary hydroxyl and benzoate groups individually examined, were as follows.

(1) The PA of isopropyl amine (915 kJ/mol) [19] is lower by 9 kJ/mol and by 10.5 kJ/mol than that *tert*-butylamine (924 kJ/mol) [19] and cyclohexyl amine (925.5 kJ/mol) [19], respectively. Thus, from these increments the PA of the methyl-2-cyclohexylamine can be estimated to be approximately 934.5 kJ/mol. Supposing that similar increments can be used to estimate PA of methyl-1-cyclohexanol from that of *ter*-butanol (810 kJ/mol) [19], which is lower by 114 kJ/mol than that of *tert*-butylamine, PA of this substituted cyclohexanol can be considered to be approximately 820.5 kJ/mol.

(2) A PA increase of 7 kJ/mol characterizes the *i*-propyl formiate ($PA_{(HCO_2iPr)}$ = 820 kJ/mol) [19] in relation to the *n*-propyl radical ($PA_{(HCO_2nPr)}$ = 813 kJ/mol) [19]. Considering that PA of propyl acetate is 839 kJ/mol) [19] then, the isopropyl acetate has a PA of about 846 kJ/mol (i.e. 839 + 7 kJ/mol). The change of acetic acid ($PA_{(CH_3COOH)}$ = 796 kJ/mol) [19] into propyl acetate corresponds to an increment increase of about 50 kJ/mol. PA of the benzoic acid being of 829 kJ/mol [19], then, isopropyl benzoate has an estimated PA of 879 kJ/mol. Alternatively, based upon the $PA_{(C_6H_5COOH)}$ value of 829 kJ/mol [19] and using the latter increment of 50 kJ/mol, PA of *i*-propyl benzoate can be estimated to be close to 879 kJ/mol (i.e. 829 + 50 kJ/mol). Furthermore, as previously emphasized from the PAs of amines, the exchange of an isopropyl radical into a cyclohexyl radical leads to an increase of 10.5 kJ/mol, and if it is assumed that a similar increment can be used for estimating PA of benzoates, thus cyclohexylbenzoate must be approximatively characterized by a PA of 889.5 kJ/mol.

References

[1] A. Mandelbaum, Mass Spectrom. Rev. 2 (1983) 223.
[2] J.S. Splitter, F. Turecek, Applications of Mass Spectrometry to Organic Stereochemistry, VCH, New York, 1994.
[3] (a) A.G. Harrison, Chemical Ionization Mass Spectrometry, 2nd ed, CRC Press, Boca Raton, FL, 1992; (b) F.J. Winkler, D. Stahl, J. Am. Chem. Soc. 101 (1979) 3685; (c) J. Bastard, D. Do Khac Manh, M. Fetizon, J.C. Tabet, D. Fraisse, J. Chem. Soc., Perkin Trans. 2 (1981) 1591.
[4] J. Respondek, H. Schwarz, F. Van Gaever, C.C. Van de Sande, Org. Mass Spectrom. 13 (1978) 618.
[5] M. Claeys, D. Van Haver, Org. Mass Spectrom. 12 (1977) 531.
[6] (a) T. Keough, Anal. Chem. 54 (1982) 2540; (b) J.J. Isbell, J.S. Brodbelt, J. Am. Soc. Mass Spectrom. 7 (1996) 565; (c) V. Gervat, F. Fournier, M.C. Perlat, J.C. Tabet, ibid. 8 (1997) 610.
[7] D.T. Leeck, T.D. Ranatunga, R.L. Smith, T. Partanen, P. Vainiotalo, H.I. Kenttämaa, Int. J. Mass Spectrom. Ion Processes 141 (1995) 229.
[8] K.K. Thoen, L. Gao, T.D. Ranatunga, P. Vainiotalo, H.I. Kenttämaa, J. Org. Chem. 62 (1997) 8702.
[9] (a) P. Tecon, Y. Hirano, C. Djerassi, Org. Mass Spectrom. 17 (1982) 277; (b) E.S. Olson, J.W. Diehl, Anal. Chem. 59 (1987) 443.
[10] A.G. Harrison, F.I. Onuska, Org. Mass Spectrom. 13 (1978) 35.
[11] (a) J.S. Brodbelt, V.H. Wysocki, R.G. Cooks, Org. Mass Spectrom. 23 (1988) 54; (b) V.H. Wysocki, D.J. Burinsky, R.G. Cooks, J. Org. Chem. 50 (1985) 1287; (c) R. Houriet, H. Rüfenacht, P.A. Carrupt, P. Vogel, M. Tichy, J. Am. Chem. Soc. 105 (1983) 3417; (d) R. Houriet, H. Rüfenacht, D. Stahl, M. Tichy, P. Longevialle, Org. Mass Spectrom. 20 (1985) 300.
[12] S. Le Meillour, J.C. Tabet, Spectrosc. Int. J. 5 (1987) 135.
[13] (a) E.S. Olson, J.W. Diehl, Anal. Chem. 59 (1987) 443; (b) J.N. Louris, R.G. Cooks, J.E.P. Syka, P.E. Kelley, G.C. Stafford Jr., J.F.J. Todd, ibid. 59 (1987) 1677; (c) J.W. Eichelberger, W.L. Budde, L.E. Slivon, ibid. 59 (1987) 2730; (d) L.K. Pannell, R.T. Pu, H.M. Fales, R.T. Mason, J.L. Stephenson, ibid. 61 (1989) 2500.
[14] (a) K. Grela, L. Konopski, J. Mass Spectrom. 30 (1995) 1441; (b) S.A. McLuckey, G.L. Glish, K.G. Asano, G.J. Van Berkel, Anal. Chem. 60 (1988) 2312; (c) N. Méchin, J. Plomley, R.E. March, T. Blasco, J.C. Tabet, Rapid. Comm. Mass Spectrom. 9 (1995) 5.

[15] N. Méchin, J. Plomley, R.E. March, T. Blasco, J.C. Tabet, Rapid. Comm. Mass Spectrom. 9 (1995) 5.
[16] E.J. Corey, J.W. Suggs, Tetrahedron Lett. 31 (1975) 2647.
[17] (a) W.J. Meyerhoffer, M.M. Bursey, Org. Mass Spectrom. 24 (1989) 169; (b) R.B. Cole, J.C. Tabet, J. Mass Spectrom. 32 (1997) 413.
[18] (a) A. Etinger, A. Idina, A. Mandelbaum, Org. Mass Spectrom. 29 (1994) 342; (b) N. Khaselev, A. Mandelbaum, J. Mass Spectrom. 30 (1995) 1533; (c) C. Denekamp, A. Mandelbaum, ibid. 30 (1995) 1421; (d) A. Etinger, A. Idina, A. Mandelbaum, J. Am. Chem. Soc. 115 (1993) 7397.
[19] S.G. Lias, J.E. Bartmess, J.F. Liebman, J.L. Holmes, R.D. Levin, W.G. Mallard, J. Phys. Chem. Ref. Data 17 (1988) Suppl. 1
[20] R.B. Cole, J.C. Tabet, Org. Mass Spectrom. 26 (1991) 59.
[21] M. Meot-Ner, Acc. Chem. Res. 17 (1984) 186.
[22] I. Jardine, C. Fenselau, J. Am. Chem. Soc. 98 (1976) 5088.
[23] (a) M. Meot-Ner, J. Am. Chem. Soc. 106 (1984) 1257; (b) W.R. Davidson, J. Sunner, P. Kebarle, ibid. 101 (1979) 1675; (c) Y.K. Lau, K. Nishizawa, A. Tse, R.S. Brown, P. Kebarle, ibid. 103 (1981) 6291; (d) M. Meot-Ner, ibid. 106 (1984) 1265.
[24] J.C. Tabet, Fundamentals of Gas Phase Ion Chemistry, K.R. Jennings (Ed.), NATO ASI Series, Kluwer Academic, The Netherlands, 1991, p. 351.
[25] (a) J. Keough, A.J. DeStefano, Org. Mass Spectrom. 16 (1981) 527; (b) J. Jalonen, J. Taskinen, C. Glidewell, Int. J. Mass Spectrom. Ion Phys. 46 (1983) 467; (c) T. Gäumann, D. Stahl, J.C. Tabet, Org. Mass Spectrom. 18 (1983) 263; (d) J.C. Beloeil, M. Bertranne, D. Stahl, J.C. Tabet, J. Am. Chem. Soc. 105 (1983) 1355; (e) J.C. Tabet, M. Bertranne, J.C. Beloeil, D. Stahl, Org. Mass Spectrom. 19 (1984) 363; (f) J.C. Promé, D. Stahl, ibid. 20 (1985) 528; (g) J.C. Tabet, H.E. Audier, J.P. Denhez, Tetrahedron 43 (1987) 873; (h) D. Despeyroux, R.B. Cole, J.C. Tabet, Org. Mass Spectrom. 27 (1992) 300; (i) T. Partanen, M. Pykäläinen, H. Hulkkonen, O. Savolainen, P. Vainiotalo, J. Chem. Soc. Perkin Trans. 2 (1994) 1743.
[26] (a) Y.Y. Lin, L.L. Smith, Biomed. Mass Spectrom. 5 (1978) 604; (b) T. Keough, A.J. DeStefano, Org. Mass Spectrom. 16 (1981) 527.
[27] (a) P. Longevialle, R. Botter, Org. Mass Spectrom. 18 (1988) 1; (b) T.H. Morton, Tetrahedron 38 (1982) 3195; (c) D.J. McAdoo, Mass Spectrom. Rev. 7 (1988) 363.
[28] (a) J.S. Brodbelt, J.N. Louris, R.G. Cooks, Anal. Chem. 59 (1987) 1278; (b) M. Soni, J. Amy, V. Frankevich, R.G. Cooks, D. Taylor, A. Mckewan, J.C. Schwartz, Rapid. Commun. Mass Spectrom. 9 (1995) 911; (c) E.J. Alvarez, J.S. Brodbelt, J. Mass Spectrom. 30 (1995) 625; (d) G.F. Bauerle Jr., B.J. Hall, N.V. Tran, J.S. Brodbelt, J. Am. Soc. Mass Spectrom. 7 (1995) 250; (e) M. Sharifi, J. Einhorm, Rapid. Commun. Mass Spectrom. 11 (1997) 1185; (f) M. Sharifi, J. Einhorm, Rapid. Commun. Mass Spectrom. 11 (1997) 727; (g) S. Gevrey, M.H. Taphanel, J.P. Morizur, J. Mass Spectrom. 33 (1998) 399.
[29] (a) R.K. Julian, M. Nappi, C. Weil, R.G. Cooks, J. Am. Soc. Mass Spectrom. 6 (1995) 57; (b) R.E. March, M.R. Weir, M. Tkaczyk, F.A. Londry, R.L. Alfred, A.M. Franklin, J.F.J. Todd, Org. Mass Spectrom. 28 (1993) 499; (c) S.A. Lammert, J.M. Wells, Rapid. Commun. Mass Spectrom. 10 (1996) 361; (d) P. Liere, T. Blasco, R.E. March, J.C. Tabet, ibid. 8 (1994) 953; (e) P. Liere, S. Bouchonnet, R.E. March, J.C. Tabet, ibid. 9 (1995) 1594; (f) P. Liere, R.E. March, T. Blasco, J.C. Tabet, Int. J. Mass Spectrom. Ion Processes 153 (1996) 101; (g) P. Liere, V. Steiner, K.R. Jennings, R.E. March, J.C. Tabet, ibid. 167/168 (1997) 735.